Platinum Thioether Macrocyclic Chemistry: Synthesis and Electrochemistry of $[PtL][PF_6]_2$ (L = [12]-, [14]- or [16]-aneS_4) and $[Pt_2([28]aneS_8)][PF_6]_4$. Crystal Structure of $[Pt([12]aneS_4)][PF_6]_2{\cdot}MeCN$†

Alexander J. Blake, Alan J. Holder, Gillian Reid and Martin Schröder*
Department of Chemistry, The University of Edinburgh, West Mains Road, Edinburgh EH9 3JJ, UK

A series of mono- and bi-nuclear platinum(II) complexes $[PtL][PF_6]_2$ (L = [12]-, [14]- or [16]-aneS_4) and $[Pt_2([28]aneS_8)][PF_6]_4$ have been synthesised by reaction of the crown thioethers with platinum(II) salts. Spectroscopic and structural data confirm square-planar homoleptic thioether co-ordination at Pt^{II} in each case. The complex $[Pt([12]aneS_4)][PF_6]_2{\cdot}MeCN$ crystallises in the orthorhombic space group *Pnma* with $a = 16.7983(9)$, $b = 9.3213(7)$, $c = 14.1954(8)$ Å and $Z = 4$. The structure shows the cation disordered over a mirror plane, with the Pt^{II} ion bound to all four thioether donors in a distorted square-planar stereochemistry, Pt–S(1) 2.266(4), Pt–S(4) 2.297(4) Å, and the metal ion lying 0.282 Å above the S_4 co-ordination plane. The methylene carbons of the macrocycle are all directed to the opposite side of the S_4 plane from the Pt^{II} ion leaving the top face of the metal centre exposed. Electrochemical studies on $[PtL]^{2+}$ show an irreversible one-electron reduction at $E_{pc} = -1.41$, -1.45 and -1.50 V *vs.* ferrocene–ferrocenium for L = [12]-, [14]- and [16]-aneS_4 respectively at a scan rate of 180 mV s^{-1}. The complex $[Pt_2([28]aneS_8)]^{4+}$ exhibits an irreversible two-electron reduction at $E_{pc} = -1.48$ V *vs.* ferrocene–ferrocenium.

The stabilisation of unusual metal oxidation-state species has been achieved for a range of transition metals (*e.g.* mononuclear Pd^{I}, Pd^{III}, Pt^{III}, Pt^{IV}, Rh^{II}, Ir^{II}, Ag^{II} and Au^{II}) by ligation to polyaza and polythia crowns.[1-8] In the course of our work we have demonstrated that macrocyclic thioether co-ordination in particular can facilitate generation of both relatively high- and low-valent metal complexes. We have observed that palladium(I) species can be generated upon co-ordination to the mixed N- and S-donor macrocyclic ligand $Me_2[18]aneN_2S_4$, in which the parent palladium(II) complex is bound through square-planar tetrathia co-ordination, with no Pd–N interaction.[2] We proposed that similar soft tetrathia platinum(II) complexes may afford mononuclear platinum(I) species upon electroreduction.

The dominance of diamagnetic Pt^{I}–Pt^{I} species in platinum(I) chemistry has been established, and reflects the strong tendency for 4d and 5d elements to form metal–metal bonded dimers.[9] There have been no well characterised examples of mononuclear platinum(I) co-ordination complexes reported in the literature. In view of this, and the paucity of polyaza and polythia macrocyclic complexes of platinum,[2,4,10,11a] we have initiated a study on the synthesis of a series of platinum(II) compounds, incorporating the thioether crowns [12]-, [14]- and [16]-aneS_4 and the potentially binucleating octathia macrocycle $[28]aneS_8$. We report herein the results of our investigation, together with a single-crystal X-ray structure determination on the platinum(II) precursor $[Pt([12]aneS_4)][PF_6]_2{\cdot}MeCN$. The results of electrochemical studies on the platinum(II) salts are also described. We have previously reported the synthesis of *cis*-$[RhCl_2([12]aneS_4)]^{+}$ in which the tetrathioether crown adopts a folded conformation at Rh^{III}.[12] During the course of this work, an alternative synthesis for $[Pt([14]aneS_4)]^{2+}$ has been reported, together with its single-crystal X-ray structure.[11a,‡]

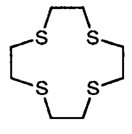

$[12]aneS_4$

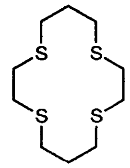

$[14]aneS_4$

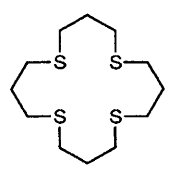

$[16]aneS_4$

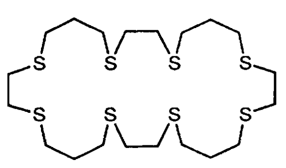

$[28]aneS_4$

Results and Discussion

Reaction of $[14]aneS_4$ or $[16]aneS_4$ (L) with 1 molar equivalent of $K_2[PtCl_4]$ in refluxing MeOH–water followed by addition of an excess of NH_4PF_6 and recrystallisation from water affords the colourless species $[Pt([14]aneS_4)][PF_6]_2$ and $[Pt([16]aneS_4)][PF_6]_2$. The composition of these species was confirmed by IR spectroscopic and microanalytical data. Additionally, the FAB mass spectra of $[PtL][PF_6]_2$ show peaks with the correct isotopic distributions corresponding to $[^{195}PtL(PF_6)]^{+}$

---

† *Supplementary data available:* see Instructions for Authors, *J. Chem. Soc., Dalton Trans.*, 1994, Issue 1, pp. xxiii–xxviii.

Ligand abbreviations: $[12]aneS_4$ = 1,4,7,10-tetrathiacyclododecane, $[14]aneS_4$ = 1,4,8,11-tetrathiacyclotetradecane, $[16]aneS_4$ = 1,5,9,13-tetrathiacyclohexadecane, $[24]aneS_8$ = 1,4,7,10,13,16,19,22-octathiacyclotetracosane, $[28]aneS_8$ = 1,4,8,11,15,18,22,25-octathiacyclooctacosane, $Me_2[18]aneN_2S_4$ = 7,16-dimethyl-7,16-diaza-1,4,10,13-tetrathiacyclooctadecane.

‡ *Note added at proof:* see also the recent publication by Endicott and co-workers.[11b]

and $[^{195}PtL]^+$. The ^1H NMR spectrum of $[Pt([14]aneS_4)]^{2+}$ recorded at 298 K in CD_3CN shows a complex second-order splitting pattern in the range δ 2.8–3.7 due to the macrocyclic protons. In contrast, the ^1H NMR spectrum of $[Pt([16]aneS_4)]^{2+}$ measured under the same conditions shows two very broad resonances centred at δ *ca.* 3.2 and 2.4. Fluxional behaviour in this system was confirmed by a variable-temperature study which shows significant sharpening of these signals upon cooling to 238 K, to give complex second-order multiplets at δ 3.28–3.06 and 2.55–2.31. These integrate as 2:1 and are assigned to the SCH_2 and $CH_2CH_2CH_2$ resonances respectively. Interestingly, both multiplets also show ^{195}Pt satellites ($I = \frac{1}{2}$, 33.0%), although $^3J_{PtH}$ and $^4J_{PtH}$ cannot be discerned due to the complexity of the signals. The ^{13}C DEPT (distortionless enhancement by polarisation transfer) NMR spectrum of $[Pt([16]aneS_4)]^{2+}$ recorded at 50.32 MHz, 298 K is also broadened, with two resonances at δ 32.96 and 24.26, which we assign to SCH_2 and $CH_2CH_2CH_2$ resonances respectively. The fluxionality in these systems probably arises from rapid flipping of the six-membered chelate rings between boat and chair conformations in solution. We have observed similar behaviour in the ^1H and ^{13}C NMR spectra of $[Pd([16]aneS_4)]^{2+}$.[13]

Travis and Busch[14] have shown previously that $[MCl_4]^{2-}$ (M = Pt or Pd) reacts with $[28]aneS_8$ to give an insoluble complex with a 4:1 metal:ligand ratio. They proposed that these products involve bidentate ligation of the macrocycle to each metal ion, with two chloride ligands completing the square-planar co-ordination geometry. Thus, in these systems $[28]aneS_8$ does not act as a binucleating ligand. However, we have recently shown that copper(I) reacts with $[28]aneS_8$ and the related $[24]aneS_8$ to form the binuclear species $[Cu_2([28]aneS_8)]^{2+}$ and $[Cu_2([24]aneS_8)]^{2+}$ respectively.[15] Single-crystal X-ray structure determinations on these both show copper(I) ions bound within the macrocyclic cavity to four thioether donors in a distorted tetrahedral geometry.[15] Very few other metal complexes of $[28]aneS_8$ have been reported.[14,16]

Reaction of $K_2[PtCl_4]$ with $[28]aneS_8$ in a 2:1 metal:ligand ratio under the same conditions described above resulted in initial formation of a yellow precipitate of $[Pt_4Cl_8([28]aneS_8)]$. However, upon prolonged refluxing this redissolved to give a pale yellow solution from which the very pale yellow complex $[Pt_2([28]aneS_8)][PF_6]_4$ could be isolated. Importantly, the IR spectrum of this product shows no Pt–Cl stretching vibration in the range 250–400 cm^{-1}. The FAB mass spectrum is also consistent with the above formulation and shows peaks with the correct isotopic distribution for $[^{195}Pt_2([28]aneS_8)(PF_6)_3]^+$ (M^+ = 1361) together with peaks corresponding to successive loss of PF_6^- counter ions. The ^1H NMR spectrum of this binuclear platinum(II) complex shows broad, second-order multiplets at δ 3.46–2.96 (SCH_2) and 2.22–1.96 ($CH_2CH_2CH_2$), while a resolution-enhanced ^{13}C DEPT NMR spectrum recorded at 300.13 MHz, 298 K indicates the presence of more than one conformational isomer in solution.

Efforts to prepare $[Pt([12]aneS_4)]^{2+}$ using the method described above proved unsuccessful with reduction to colloidal platinum(0) predominating. This is presumably a result of the size mis-match between the relatively large platinum(II) ion and the small 12-membered tetrathia crown. Consequently, complexation is much more difficult than for the larger ring sizes, and reduction to platinum metal occurs more readily under the conditions used. Complexation was successfully achieved by treatment of $PtCl_2$ with 1 molar equivalent of $[12]aneS_4$ in refluxing MeCN, generating a bright yellow precipitate within *ca.* 2 h. Introduction of water to the reaction at this stage resulted in complete dissolution of the precipitate. After cooling, excess NH_4PF_6 was added and the reaction volume reduced to afford a yellow precipitate of $[Pt([12]aneS_4)][PF_6]_2$. This formulation was confirmed by IR spectroscopic and microanalytical data. Additionally, the FAB mass spectrum of the compound showed peaks with the correct isotopic distributions at M^+ 579 and 435 which were assigned to $[^{195}Pt([12]aneS_4)(PF_6) - H]^+$ and $[^{195}Pt([12]aneS_4)]^+$ respectively. The ^1H NMR spectrum of the complex recorded in CD_3CN at 298 K shows (Fig. 1) essentially an AA′BB′ splitting pattern at δ 3.95–3.26 arising from the macrocyclic protons, while the ^{13}C DEPT NMR exhibits a single resonance at δ 38.99, indicating that all eight macrocyclic carbon atoms are equivalent in solution. These data are consistent with a square-planar $[Pt([12]aneS_4)]^{2+}$ cation. In order to confirm the geometry of the complex and to investigate the conformation of the macrocyclic ligand, a single-crystal X-ray structure determination was undertaken.

Suitable crystals were obtained by slow diffusion of diethyl ether vapour into a solution of the complex in MeCN. A structure determination on $[Pt([12]aneS_4)][PF_6]_2 \cdot MeCN$ shows (Fig. 2) the cation occupying a crystallographic mirror plane, with the macrocycle disordered over this mirror, such that the individual cations do not exhibit *m*-symmetry. The first component of the disorder is defined by the atoms C(12B), S(1), C(2), C(3), S(4) and C(5); the second by C(12), S(1), C(2B), C(3), S(4) and C(5B). Each ring is formed by linking one component of the disorder to the mirrored equivalent of the other component. Thus C(5) is the mirror equivalent of C(5′) but is actually bonded to C(5D); C(5B) is related to C(5D) but is bonded to C(5′). A similar relationship relates C(12), C(12′), C(12D) and C(12B).*

The metal ion is co-ordinated to a distorted square planar arrangement of all four macrocyclic S-donors, Pt–S(1) 2.266(4), Pt–S(4) 2.297(4) Å. The angles around Pt^{II} are slightly less than 90°, and the S(1)–Pt–S(4′) angle of 165.77(14)° reflects the restricted bite angle of the $SCH_2CH_2SCH_2CH_2S$ linkage, and the poor size-match between the Pt^{II} ion and the available cavity of the 12-membered ring. The Pt^{II} ion is displaced by 0.282 Å from the S_4 co-ordination plane, with the methylene chains all directed to the opposite side from the metal ion. As a result, one face of the metal is completely exposed, the nearest approach to the metal being 3.780 Å by N(1S) of MeCN (at $\frac{1}{2} - x, -\frac{1}{2} + y,$

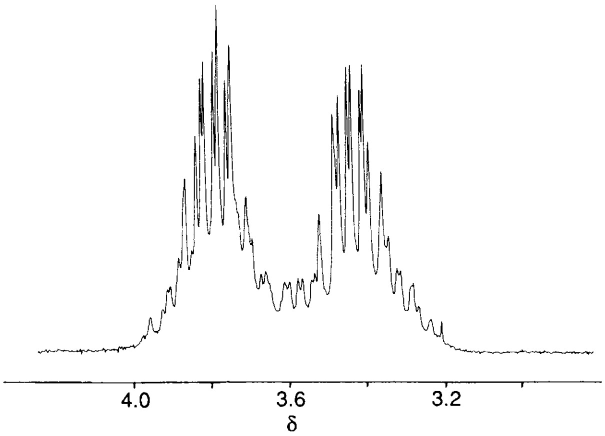

Fig. 1 Proton NMR spectrum of $[Pt([12]aneS_4)][PF_6]_2$ (200.13 MHz, CD_3CN, 298 K)

---

* The cation is disordered about a crystallographic mirror plane at $y = \frac{1}{4}$ which passes through the metal and relates S(1)–C(2)–C(3)–S(4) to S(1′)–C(2′)–C(3′)–S(4′). The disorder may be described in terms of two alternative routes between the mirror pairs of S atoms: the individual components of the disorder, one of which is shown in Fig. 2, do not conform to the mirror symmetry. Thus, C(5) is bonded to the mirror equivalent, C(5D), of its alternative, C(5B), which in turn links to C(5′), the alternative to C(5D). A similar description applies to the pairs C(12)/C(12D) and C(12B)/C(12′). This model avoids the unfavourable eclipsing of C–H bonds across the mirror plane which would result if the components were to obey mirror symmetry.

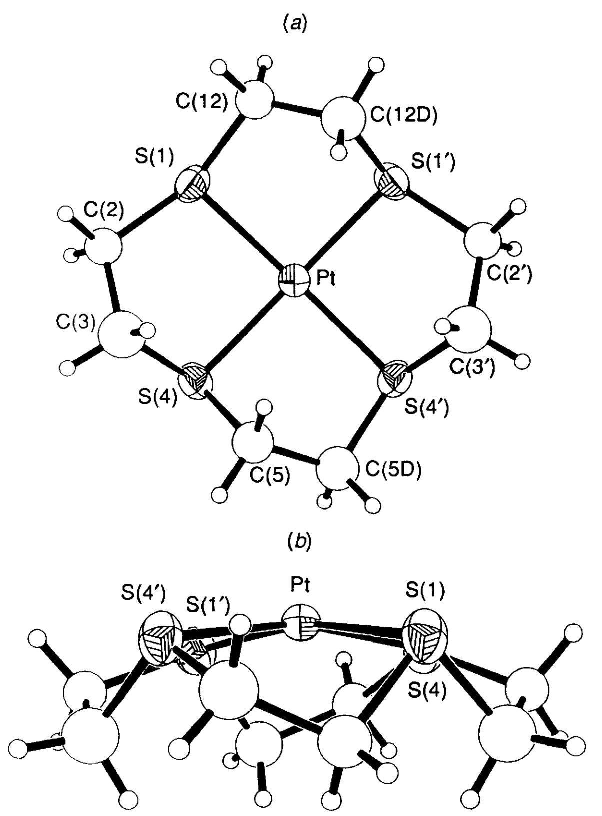

Fig. 2 (*a*) View of one of the two equally-occupied conformers of $[Pt([12]aneS_4)]^{2+}$ and (*b*) edge view of $[Pt([12]aneS_4)]^{2+}$ showing the conformation of the macrocycle in one component of the disorder

$-\frac{1}{2} + z$). We have observed a similar conformation for the related palladium(II) complexes $[Pd([12]aneS_4)]^{2+}$ and $[Pd([14]aneS_4)]^{2+}$,[1,13] and Endicott and co-workers[11a] have reported a similar structure for $[Pt([14]aneS_4)]^{2+}$, in which the S-atom lone pairs are also all up. However, in the latter case the Pt ion occupies the best S_4-plane as a result of the larger cavity available in the 14-membered crown.[11a]

The ability of $[12]aneS_4$ to co-ordinate in a square-planar arrangement to Pt^{II} and Pd^{II} in $[M([12]aneS_4)]^{2+}$ is remarkable; in comparison, for the complexes $[RhCl_2L]^+$ a *trans*-dichloro geometry is formed for L = $[16]aneS_4$, while for the 12- and 14-membered thiacrowns a folded, *cis*-dichloro arrangement occurs exclusively.[12] Likewise, $[Pd([16]aneS_4)]^{2+}$ shows Pd^{II} sited within the least-squares S_4 plane.[1,13]

Electrochemistry.—Cyclic voltammetry of $[PtL][PF_6]_2$ measured in MeCN at 298 K (0.1 mol dm^{-3} NBu_4PF_6 supporting electrolyte) shows an irreversible reduction at $E_{pc} = -1.41$, -1.45 or -1.50 V *vs.* ferrocene–ferrocenium for L = [12]-, [14]- or [16]-aneS_4 respectively at a scan rate of 180 mV s^{-1}. The reduction peaks shift to more negative potential with increasing scan rate. Coulometric measurements were performed in an attempt to quantify the number of electrons associated with these processes. For $[Pt([12]aneS_4)]^{2+}$ these measurements were inhibited due to plating of Pt metal on the platinum basket working electrode. This is consistent with reduction to Pt^0 with concomitant demetallation due to the relatively small cavity size of $[12]aneS_4$. We have observed similar electrochemical behaviour for $[Pd([12]aneS_4)]^{2+}$. In this case, however, demetallation could be inhibited by reducing the temperature to *ca.* 273 K, and coulometric measurements at this temperature confirmed the reduction to be a one-electron process.[13]

The reductions of $[Pt([14]aneS_4)]^{2+}$ and $[Pt([16]aneS_4)]^{2+}$ are each one-electron processes (n = 0.92 and 1.02 respectively by coulometry) to generate yellow solutions. However, these solutions showed no ESR signal (measured at 77 K as a MeCN glass). Similarly, $[Pt_2([28]aneS_8)][PF_6]_4$ exhibits a broad, irreversible two-electron reduction at *ca.* -1.48 V *vs.* ferrocene–ferrocenium, to give a yellow, ESR silent solution. These results suggest that while reduction of these platinum(II) thioether complexes occur at relatively accessible potentials, any platinum(I) radical species generated are transient and are quenched rapidly, possibly *via* direct Pt^I–Pt^I bond formation. Further studies using thioether macrocycles which incorporate bulky organic groups on the carbon backbone and hence inhibit direct metal–metal bond formation may help to confirm whether thioether co-ordination does indeed stabilise d^9 platinum(I) radicals.

Experimental

Infrared spectra were measured as KBr and CsI discs using a Perkin-Elmer 598 spectrometer over the range 200–4000 cm^{-1}. Electrochemical measurements were performed on a Bruker E310 Universal Modular Polarograph. All readings were taken using a three-electrode potentiostatic system in acetonitrile containing 0.1 mol dm^{-3} NBu_4PF_6 or NBu_4BF_4 as supporting electrolyte. Cyclic voltammetric measurements were carried out using a double platinum electrode and a Ag–AgCl reference electrode. All potentials are quoted *versus* ferrocene–ferrocenium. Electronic spectra were measured in quartz cells using a Perkin-Elmer Lambda 9 spectrophotometer. Mass spectra were run by electron impact on a Kratos MS902 and by fast atom bombardment using 3-nitrobenzyl alcohol (noba) as matrix on a Kratos MS 50TC spectrometer.

Syntheses.—$[Pt([12]aneS_4)][PF_6]_2$. Platinum(II) dichloride (44 mg, 0.166 mmol) was added to a solution of $[12]aneS_4$ (40 mg, 0.166 mmol) in MeCN (40 cm^3). The reaction mixture was refluxed for 2 h to give a bright yellow precipitate. Upon addition of water (40 cm^3) this solid redissolved. The resulting pale yellow solution was refluxed for a further 6 h. After cooling and filtering, an excess of NH_4PF_6 was added giving a yellow solid which was collected by filtration, recrystallised from MeCN–diethyl ether and dried *in vacuo*. Yield: 63% (Found: C, 13.8; H, 2.25; S, 17.9. $C_8H_{16}F_{12}P_2PS_4$ requires C, 13.3; H, 2.20; S, 17.7%. FAB mass spectrum (noba matrix): *m/z* 579, 435; calc. for $[^{195}Pt([12]aneS_4)PF_6]^+$ 580, $[^{195}Pt([12]aneS_4)]^+$ 435. NMR (CD_3CN, 298 K): ^1H (200.13 MHz), δ 3.95–3.26 (AA′BB′ pattern, CH_2, 16 H); ^{13}C DEPT (50.32 MHz), δ 38.99 (CH_2, 8 C). IR (KBr disc): 2980w, 2920m, 2840w, 1440w, 1410w, 1380m, 1305w, 1190w, 1175w, 1130w, 940w, 840vs, 740w, 660w, 625w and 555vs cm^{-1}.

$[Pt([14]aneS_4)][PF_6]_2$.—Reaction of $K_2[PtCl_4]$ (120 mg, 0.289 mmol) with $[14]aneS_4$ (85 mg, 0.317 mmol) in refluxing water–MeOH (1 : 1 v/v, 20 cm^3) for 4 h gave a near colourless solution. Addition of excess NH_4PF_6 afforded a white precipitate which was recrystallised from water and dried *in vacuo*. Yield: 60% (Found: C, 15.9; H, 2.65. $C_{10}H_{20}F_{12}P_2PtS_4$ requires C, 15.9; H, 2.70%). FAB mass spectrum (noba matrix): *m/z* = 609, 464; calc. for $[^{195}Pt([14]aneS_4)PF_6]^+$, 608 $[^{195}Pt([14]aneS_4)]^+$ 463. ^1H NMR (80.13 MHz, CD_3CN, 298 K): δ 3.7–2.8 (CH_2, 20 H). IR (KBr disc): 3000w, 2940m, 2910w, 2885w, 1430w, 1410w, 1290m, 1210w, 1140w, 940w, 840vs, 740w, 660w and 555vs cm^{-1}.

$[Pt([16]aneS_4)][PF_6]_2$. Procedure as above, using $K_2[PtCl_4]$ (56 mg, 0.135 mmol) and $[16]aneS_4$ (40 mg, 0.135 mmol). The product was isolated as a white microcrystalline solid. Yield: 73% (Found: C, 18.5; H, 3.10; S, 16.3. $C_{12}H_{24}F_{12}P_2PtS_4$ requires C, 18.4; H, 3.10; S, 16.3%). FAB mass spectrum (noba matrix): *m/z* 636, 490; calc. for $[^{195}Pt([16]aneS_4)PF_6]^+$ 636, $[^{195}Pt([16]aneS_4)]^+$ 491. NMR (CD_3CN, 298 K): ^1H (360.13 MHz), δ 3.28–3.08

Table 1 Selected bond lengths (Å), angles (°) and torsion angles for $[Pt([12]aneS_4)][PF_6]_2{\cdot}MeCN$ estimated standard deviations (e.s.d.s) in parentheses

Pt–S(1)	2.266(4)	Pt–S(4)	2.297(4)
S(1)–Pt–S(4)	89.13(14)	S(4)–C(3)–C(2B)	117.4(13)
S(1)–Pt–S(1′)	89.67(14)	Pt–S(4)–C(3)	98.4(5)
S(1)–Pt–S(4′)	165.77(14)	Pt–S(4)–C(5)	92.8(9)
S(4)–Pt–S(4′)	88.55(13)	Pt–S(4)–C(5B)	101.3(10)
C(12B)–C(12′)–S(1′)	120.1(18)	C(3)–S(4)–C(5)	92.9(10)
C(12′)–C(12B)–S(1)	103.6(17)	C(3)–S(4)–C(5B)	115.1(11)
Pt–S(1)–C(12B)	96.8(8)	S(4)–C(5)–C(5D)	108.8(20)
Pt–S(1)–C(2)	101.1(7)	S(4′)–C(5′)–C(5B)	108.8(20)
Pt–S(1)–C(12)	97.7(8)	S(1′)–C(12D)–C(12)	103.6(17)
Pt–S(1)–C(2B)	95.3(8)	S(1)–C(12)–C(12D)	120.1(18)
C(12B)–S(1)–C(2)	112.1(11)	S(1)–C(2B)–C(3)	117.4(16)
C(12)–S(1)–C(2B)	107.8(12)	S(4)–C(5B)–C(5′)	111.1(21)
S(1)–C(2)–C(3)	117.4(14)	C(5)–C(5D)–S(4′)	111.1(21)
C(2)–C(3)–S(4)	107.1(11)		
S(1′)–C(12′)–C(12B)–S(1)	−53.1(22)	C(2)–C(3)–S(4)–C(5)	146.1(14)
C(12′)–C(12B)–S(1)–C(2)	161.6(15)	C(2B)–C(3)–S(4)–C(5B)	123.3(17)
C(12B)–S(1)–C(2)–C(3)	−82.0(17)	S(4)–C(3)–C(2B)–S(1)	18.3(22)
C(2B)–S(1)–C(12)–C(12′)	112.2(28)	C(3)–S(4)–C(5)–C(5D)	−162.0(19)
C(2B)–S(1)–C(12)–C(12B)	8.6(30)	C(3)–S(4)–C(5B)–C(5′)	−84.2(22)
C(2B)–S(1)–C(12)–C(12D)	80.0(21)	S(4)–C(5)–C(5D)–S(4′)	59.7(23)
C(12)–S(1)–C(2B)–C(3)	−142.2(17)	S(4′)–C(5′)–C(5B)–S(4)	− 59.7(23)
S(1)–C(2)–C(3)–S(4)	−51.3(16)	S(1′)–C(12D)–C(12)–S(1)	53.1(22)

Table 2 Atomic coordinates for $[Pt([12]aneS_4)][PF_6]_2{\cdot}MeCN$ with e.s.d.s in parentheses

Atom	*x*	*y*	*z*
Pt	0.165 02(4)	0.250 0	0.126 06(5)
S(1)	0.097 71(21)	0.078 6(4)	0.206 5(3)
S(4)	0.253 55(23)	0.078 0(4)	0.076 6(3)
P(1)	0.373 1(3)	0.250 0	0.424 6(4)
F(11)	0.463 5(4)	0.250 0	0.402 1(12)
F(12)	0.388 3(7)	0.368 6(17)	0.499 0(12)
F(13)	0.284 0(6)	0.250 0	0.453(3)
F(14)	0.361 5(8)	0.367 8(17)	0.348 8(11)
P(2)	−0.027 2(3)	0.750 0	0.393 9(4)
F(21)	0.055 1(6)	0.750 0	0.344 6(13)
F(22)	−0.054 6(9)	0.869 4(15)	0.325 2(10)
F(23)	−0.109 5(9)	0.750 0	0.443 3(19)
F(24)	0.005 6(10)	0.860 0(17)	0.466 0(10)
N(1S)	0.285 9(19)	0.750 0	0.366 2(16)
C(1S)	0.349 6(19)	0.750 0	0.374 4(17)
C(2S)	0.433 5(24)	0.750 0	0.394 0(19)
C(12′)	0.061 3(18)	0.310 2(23)	0.299 4(15)
C(12B)	0.099 8(18)	0.166 (3)	0.318 5(12)
C(2)	0.166 1(7)	−0.067 6(15)	0.200 5(22)
C(3)	0.252 6(8)	−0.032 3(18)	0.179 4(9)
C(5)	0.337 5(13)	0.179 (3)	0.116 3(24)
C(5′)	0.337 5(13)	0.321(3)	0.116 3(24)
C(12D)	0.099 8(18)	0.334(3)	0.318 5(12)
C(12)	0.061 3(18)	0.189 8(23)	0.299 4(15)
C(2B)	0.184 5(10)	−0.011(4)	0.248 5(14)
C(5B)	0.341 7(12)	0.182(3)	0.061(3)
C(5D)	0.341 7(12)	0.318(3)	0.061(3)

(SCH_2, 16 H) and 2.55–2.31 ($CH_2CH_2CH_2$, 8 H); ^{13}C DEPT (50.32 MHz), two broad resonances at δ 32.96 (SCH_2) and 24.26 ($CH_2CH_2CH_2$). IR (KBr disc): 3000m, 2920m, 2845w, 1440m, 1420m, 1380w, 1300m, 1290w, 1260w, 1245w, 1200w, 1125w, 1025w, 840vs, 770m, 740w and 555vs cm^{-1}.

$[Pt_2([28]aneS_8)][PF_6]_4$. Method as above, using $K_2[PtCl_4]$ (155 mg, 0.372 mmol) and $[28]aneS_8$ (100 mg, 0.186 mmol). The product was isolated as a pale yellow solid. Yield: 48% (Found: C, 16.3; H, 2.75; S, 16.4. $C_{20}H_{40}F_{24}P_4Pt_2S_8$ requires C, 15.9; H, 2.70; S, 17.0%). FAB mass spectrum (noba matrix): *m/z* 1361, 1250, 1232, 1212, 1105, 1089, 1069; calc. for $[^{195}Pt_2([28]aneS_8)(PF_6)_3]^+$ 1361, $[^{195}Pt_2([28]aneS_8)(PF_6)_2{\cdot}2H_2O]^+$ 1252, $[^{195}Pt_2([28]aneS_8)(PF_6)_2{\cdot}H_2O]^+$ 1234, $[^{195}Pt_2([28]aneS_8)(PF_6)_2]^+$ 1216, $[^{195}Pt_2([28]aneS_8)(PF_6){\cdot}2H_2O]^+$ 1107, $[^{195}Pt_2([28]aneS_8)(PF_6){\cdot}H_2O]^+$ 1089, $[^{195}Pt_2([28]aneS_8)(PF_6)]^+$ 1071. NMR (CD_3CN, 298 K): ^1H (360.13 MHz), δ 3.46–2.96 (SCH_2, 32 H) and 2.22–1.96 ($CH_2CH_2CH_2$, 8 H); ^{13}C DEPT (300.13 MHz), δ 40.24, 38.46, 37.25, 36.73, 36.49, 36.30, 35.67, 35.13, 33.83, 33.61, 33.12 (SCH_2), 25.29, 23.23 and 23.07 ($CH_2CH_2CH_2$). IR (KBr disc): 2960m, 2900w, 1500w, 1420m, 1300m, 1250m, 1200m, 1170m, 840vs and 555vs cm^{-1}.

Structure Determination of $[Pt([12]aneS_4)][PF_6]_2{\cdot}MeCN$.—Slow diffusion of diethyl ether vapour into a solution of the complex in MeCN gave pale yellow needles of adequate diffraction quality. The selected crystal (0.096 × 0.096 × 0.92 mm) was sealed in a glass capillary to prevent solvent loss.

Crystal data. $C_8H_{16}F_{12}P_2PtS_4{\cdot}CH_3CN$, $M = 766.43$, orthorhombic, space group *Pnma*, with $a = 16.7983(9)$, $b = 9.3213(7)$, $c = 14.1954(8)$ Å, $U = 2222.7$ Å^3 [from 2θ values of 58 reflections measured at ± ω (2θ = 30–32°, $\bar{\lambda} = 0.710\ 73$ Å)], $Z = 4$, $D_c = 2.290$ g cm^{-3}, $T = 298$ K, $\mu = 6.978$ mm^{-1}, $F(000) = 1464$.

Data collection and processing. Stoë STADI-4 four-circle diffractometer, graphite-monochromated Mo-Kα X-radiation, ω–2θ scans using the learnt-profile method,[17] 1653 data ($2\theta_{max}$ 45°, *h* 0–18, *k* 0–10, *l* 0–15), semiempirical absorption correction (min. 0.2106, max. 0.2535) applied, giving 1213 reflections with $F \geqslant 6\sigma(F)$ for use in all calculations. No significant crystal decay or movement was observed.

Structure solution and refinement. A Patterson synthesis revealed the Pt ion occupying a site of *m* symmetry. Subsequent iterative cycles of least-squares and difference-Fourier analysis[18] located all other non-H atoms for one half molecule. The two PF_6^- counter ions also occupy sites of *m* symmetry, with one F–P–F axis lying along the mirror. One MeCN solvent molecule was found to be associated with each $[Pt([12]aneS_4)]^{2+}$ cation, and this also lies on a mirror plane at $y = \frac{3}{4}$. During refinement two distinct, equally-occupied conformations of the $[Pt([12]aneS_4)]^{2+}$ cation could be discerned. Systematic absences indicated the space group to be either $Pn2_1a$ or *Pnma*. The initial solution in *Pnma* located all non-H atoms satisfactorily, with the exception of the macrocyclic methylene carbons which appeared to be affected by disorder. Refinement in *Pn*2_1*a* also indicated the presence of disorder and therefore offered no advantages. We persisted with a disorder model in *Pnma*: by allowing the carbon atoms to be disordered across the mirror plane we were able to rationalise the disorder in terms of cations with only approximate mirror symmetry lying on crystallographic mirror planes. The two forms were modelled successfully by constraining the macrocyclic C–C and C–S bond lengths to be 1.52 and 1.785(8) Å respectively. Careful analysis of the intraligand bond angles, as well as the residual errors from this model compared to the alternative in which the cation possesses genuine *m* symmetry, led to the conclusion that while the complex crystallises in space group *Pnma* with *m* symmetry, neither of the individual conformations of the macrocyclic cation possesses *m* symmetry. This conclusion is also intuitively sensible as it precludes the unrealistic situation of having CH_2 groups eclipsed across the mirror. At isotropic convergence final corrections for absorption were made using DIFABS.[19] All fully-occupied non-hydrogen atoms were refined anisotropically. Hydrogen atoms were included at fixed, calculated positions. At final convergence R, R' = 0.0489, 0.0678 respectively, S = 1.214 for 147 refined parameters and the final ΔF synthesis showed no peak above 1.48 (close to Pt) or below −1.05 e Å^{-3}. The weighting scheme $w^{-1} = \sigma^2(F) + 0.000\,218\,F^2$ gave satisfactory agreement analyses and in the final cycle $(\Delta/\sigma)_{max}$ was 0.01. Atomic scattering factors were inlaid,[18] or taken from ref. 20. Molecular geometry calculations utilised CALC[21] and the Figures were produced by SHELXTL PC.[22] Selected bond lengths, angles and torsion angles are given in Table 1. Fractional atomic coordinates are listed in Table 2.

Additional material available from the Cambridge Crystallographic Data Centre comprises H-atom coordinates, thermal parameters and remaining bond lengths and angles.

Acknowledgements

We thank the SERC for support, the Royal Society of Edinburgh and Scottish Office Education Department for a Support Research Fellowship (to M.S.), and Johnson-Matthey plc for generous loans of platinum. We also thank Dr. David Reed and Mr. J. R. A. Miller for their help with NMR studies for this work.

References

1 M. Schröder, *Pure Appl. Chem.*, 1988, **60**, 517; A. J. Blake and M. Schröder, *Adv. Inorg. Chem.*, 1990, **35**, 1; G. Reid and M. Schröder, *Chem. Soc. Rev.*, 1990, **19**, 239; S. R. Cooper and S. C. Rawle, *Struct. Bonding (Berlin)*, 1990, **72**, 1; K. Wieghardt and P. Chaudhuri, *Prog. Inorg. Chem.*, 1987, **35**, 329.

2 A. J. Blake, R. O. Gould, T. I. Hyde and M. Schröder, *J. Chem. Soc., Chem. Commun.*, 1987, 431; 1730; G. Reid, A. J. Blake, T. I. Hyde and M. Schröder, *J. Chem. Soc., Chem. Commun.*, 1988, 1397; A. J. Blake, G. Reid and M. Schröder, *J. Chem. Soc., Dalton Trans.*, 1990, 3363.

3 A. J. Blake, L. M. Gordon, A. J. Holder, T. I. Hyde, G. Reid and M. Schröder, *J. Chem. Soc., Chem. Commun.*, 1988, 1452; G. Hunter, A. McAuley and T. W. Whitcombe, *Inorg. Chem.*, 1988, **27**, 2634; A. McAuley and T. W. Whitcombe, *Inorg. Chem.*, 1988, **27**, 3090; A. J. Blake, A. J. Holder, T. I. Hyde, Y. V. Roberts, A. J. Lavery and M. Schröder, *J. Organomet. Chem.*, 1987, **323**, 261; A. J. Blake, R. O. Gould, A. J. Lavery and M. Schröder, *Angew. Chem.*, 1986, **98**, 282; *Angew. Chem., Int. Ed. Engl.*, 1986, **25**, 274; G. J. Grant, K. A. Sanders, W. N. Setzer and D. G. VanDerveer, *Inorg. Chem.*, 1991, **30**, 4053.

4 A. J. Blake, R. O. Gould, A. J. Holder, T. I. Hyde, M. O. Odulate, A. J. Lavery and M. Schröder, *J. Chem. Soc., Chem. Commun.*, 1987, 118; K. Wieghardt, M. Koppen, W. Swiridoff and J. Weiss, *J. Chem. Soc., Dalton Trans.*, 1983, 1869.

5 A. J. Blake, R. O. Gould, A. J. Holder, T. I. Hyde and M. Schröder, *J. Chem. Soc., Dalton Trans.*, 1988, 1861; S. C. Rawle, R. Yagbasan, K. Prout and S. R. Cooper, *J. Am. Chem. Soc.*, 1987, **109**, 6181; S. R. Cooper, S. C. Rawle and R. Yagbasan, *J. Am. Chem. Soc.*, 1991, **113**, 1600; D. Collison, G. Reid and M. Schröder, *Polyhedron*, 1992, **11**, 3165.

6 A. J. Blake, R. O. Gould, A. J. Holder, T. I. Hyde, G. Reid and M. Schröder, *J. Chem. Soc., Dalton Trans.*, 1990, 1759.

7 A. J. Blake, G. Reid and M. Schröder, *J. Chem. Soc., Dalton Trans.*, 1991, 615; A. J. Blake, R. O. Gould, A. J. Holder, T. I. Hyde and M. Schröder, *Polyhedron*, 1989, **8**, 513; A. J. Blake, R. O. Gould, C. Radek, G. Reid, A. Taylor and M. Schröder, *Proceedings of the 1st International Conference on the Chemistry of the Copper and Zinc Triads*, Royal Society of Chemistry, Edinburgh, 1992; A. J. Blake, D. Collison, R. O. Gould, G. Reid and M. Schröder, *J. Chem. Soc., Dalton Trans.*, 1993, 521.

8 A. J. Blake, R. O. Gould, J. A. Greig, A. J. Holder, T. I. Hyde and M. Schröder, *J. Chem. Soc., Chem. Commun.*, 1989, 876; A. J. Blake, J. A. Greig, A. J. Holder, T. I. Hyde, A. Taylor and M. Schröder, *Angew. Chem.*, 1990, **102**, 203; *Angew. Chem., Int. Ed. Engl.*, 1990, **29**, 197.

9 D. M. Roundhill, *Comprehensive Co-ordination Chemistry*, eds. G. Wilkinson, J. A. McCleverty and R. D. Gillard, vol. 5, ch. 52, Pergamon, Oxford, 1987; V. K. Jain, *Rev. Inorg. Chem.*, 1988, **9**, 299.

10 E. Kimura, Y. Lin, R. Machida and H. Zenda, *J. Chem. Soc., Chem. Commun.*, 1986, 1020; E. Kimura, S. Korenari, M. Shionoya and M. Shiro, *J. Chem. Soc., Chem. Commun.*, 1988, 1166; A. J. Blake, G. Reid and M. Schröder, *Acta Crystallogr., Sect. C*, 1991, **47**, 64; R. McCrindle, G. Ferguson, A. J. McAlees, M. Parvez, B. L. Ruhl, D. K. Stephenson and T. Wieckowski, *J. Chem. Soc., Dalton Trans.*, 1986, 2351; A. J. Jircitano, M. D. Timken, K. B. Mertes and J. R. Ferraro, *J. Am. Chem. Soc.*, 1979, **101**, 7661; S. Brawner and K. B. Merks, *J. Inorg. Nucl. Chem.*, 1979, **41**, 764.

11 (*a*) D. Waknine, M. J. Heeg, J. F. Endicott and L. A. Ochrymowycz, *Inorg. Chem.*, 1991, **30**, 3691; (*b*) M. A. Watzky, D. Waknine, M. J. Heeg, J. F. Endicott and L. A. Ochrymowycz, *Inorg. Chem.*, 1993, **32**, 4882.

12 A. J. Blake, G. Reid and M. Schröder, *J. Chem. Soc., Dalton Trans.*, 1989, 1675.

13 A. J. Blake, A. J. Holder, G. Reid and M. Schröder, unpublished work.

14 K. Travis and D. H. Busch, *Chem. Commun.*, 1970, 1041.

15 A. J. Blake, A. Taylor and M. Schröder, *Polyhedron*, 1990, **9**, 2919.

16 R. E. DeSimone and T. M. Tighe, *J. Inorg. Nucl. Chem.*, 1976, **38**, 1623; D. Sevdić and H. Meider, *J. Inorg. Nucl. Chem.*, 1977, **39**, 1403; A. C. Braithwaite, C. E. F. Rickard and T. N. Waters, *Aust. J. Chem.*, 1981, **34**, 2665; K. Saito, Y. Masudo and E. Sekido, *Anal. Chim. Acta*, 1983, **151**, 447; A. J. Blake, A. Taylor and M. Schröder, *J. Chem. Soc., Chem. Commun.*, 1993, 1097.

17 W. Clegg, *Acta Crystallogr., Sect. A*, 1981, **37**, 22.

18 G. M. Sheldrick, SHELX 76, program for crystal structure refinement, University of Cambridge, 1976.

19 DIFABS, program for empirical absorption corrections, N. Walker and D. Stuart, *Acta Crystallogr., Sect. A*, 1983, **39**, 158.

20 D. T. Cromer and J. B. Mann, *Acta Crystallogr., Sect. A*, 1968, **24**, 321.

21 R. O. Gould and P. Taylor, CALC, program for molecular geometry calculations, University of Edinburgh, 1985.

22 G. M. Sheldrick, SHELXTL PC version 4.2, University of Göttingen, 1989.

Received 18*th May* 1993; *Paper* 3/06029B